

Electron Exchange between Amphiphilic 4-Alkylpyridinepentaammineruthenium Ions Separated by Phospholipid Vesicle Bilayers

Lester Y. C. Lee and James K. Hurst*

Contribution from the Department of Chemical, Biological, and Environmental Sciences, Oregon Graduate Center, Beaverton, Oregon 97006. Received May 9, 1984

Abstract: Gel exclusion chromatography and optical spectroscopy were used to demonstrate that the $(\text{NH}_3)_5\text{Ru}-4-(11'\text{-dodecyl})\text{pyridine}(3+)$ ion binds to unilamellar phosphatidylcholine liposomes; ions containing shorter ω -alkenyl substituents show progressively weaker binding with decreasing chain length. Addition of chromous, vanadous, or ascorbate ions to the vesicle suspensions gives rise to biphasic one-electron reduction of the bound $(\text{NH}_3)_5\text{Ru}-4-(11'\text{-dodecyl})\text{pyridine}(3+)$ ion. The slow-phase step is observed only if the Ru(III) ion is initially bound to both inner and outer vesicle surfaces. About 30% of the total reaction proceeds by this step, which corresponds to the proportion of area comprising the inner vesicle surface. Slow-phase reduction follows first-order kinetics, with $k = 10^{-3} \text{ s}^{-1}$ at 23 °C, independent of the concentration and identity of added reducing agent. The reduction rate is unaffected by incorporating either the potassium ionophore, valinomycin, or the proton carrier, carbonyl cyanide *m*-chlorophenylhydrazone, into the liposomes. No evidence for transmembrane diffusion of external reducing agents or liposome-bound Ru(II) or Ru(III) ions occurring on the time scale of the slow-phase reduction could be found. These results suggest that the reaction step involves rate-limiting electron exchange between $(\text{NH}_3)_5\text{Ru}-4-(11'\text{-dodecyl})\text{pyridine}(2+/3+)$ ions located on the opposite vesicle surfaces. The electron-transfer rate is consistent with a hopping conduction model in which electrons tunnel to intermediary sites located within the hydrocarbon phase at the bilayer alkyl chain interface.

Long-range electron transfer, i.e., occurring over distances greater than closest approach of the reactant ions and molecules, has now been demonstrated in a wide variety of chemical and biochemical systems.^{1,2} The principles governing these reactions are not well understood. For example, electron transfer from cytochrome *c*₂ to the bacteriochlorophyll dimer in the *C. vinosum* photoreduction center shows a complex temperature profile³ that is adequately rationalized by vibronically assisted electron tunneling models.^{4,5} In contrast, electron transfer to the ferrihem in cytochrome *c* from a peripherally bound imidazole-pentaammineruthenium(II) ion is temperature independent under ambient conditions,^{2b,c} implying the absence of vibronic coupling between the redox sites (see, however, ref 5 c). In both systems, separation between the metal centers is of the order of 10 Å and other structural features are at least grossly similar, so there is presently no apparent basis for their markedly disparate kinetic behavior.

As an approach to the general problem, we are investigating mechanisms of oxidation-reduction across bilayer membranes where systematic variation of barrier properties is possible. Several reports have appeared describing transmembrane redox in asymmetrically organized vesicles.⁶⁻¹¹ In a liposomal system comprising

phospholipid-bound amphiphilic $\text{Ru}(\text{bpy})_3^{2+/3+}$ derivatives with internally compartmented EDTA and externally added alkylviologens, photostimulated viologen reduction was interpreted in terms of rate-limiting electron exchange between the $\text{Ru}(\text{bpy})_3^{2+/3+}$ ions bound at the opposite interfaces.⁶ Similarly, in dihexadecyl phosphate (DHP) vesicles containing $\text{Ru}(\text{bpy})_3^{2+}$ and methylviologen ions bound to opposite surfaces, oxidative quenching of the photoexcited ruthenium complex was thought to occur by transmembrane electron transfer,⁷ although it is now recognized that photoexcitation of DHP-bound chromophores promotes transmembrane diffusion of the electron acceptor, so that reaction in this instance is a consequence of viologen migration followed by reaction with photosensitizer bound to the same surface.¹² To avoid potential complications associated with photostimulated diffusion, we have sought to develop microphase-separated redox systems that are not driven by photoexcitation. In the present study, we examine the reduction of (phosphatidylcholine liposome)-bound 4-(11'-dodecyl)pyridinepentaammineruthenium(III) ion by externally added reducing agents; the redox kinetics support our conclusion that transmembrane reduction occurs by rate-limiting electron transfer across the bilayer.

Experimental Section

Reagents. Lecithin was isolated from hens' eggs by solvent extraction and chromatography on alumina;¹³ the purified product gave a single spot when chromatographed on silica gel TLC plates.¹³ The purified phosphatidylcholine was suspended in distilled water and kept frozen until used.

Alkylpyridine compounds used as ligands were prepared and purified as previously described;¹⁴ product structures were confirmed by ¹H NMR analysis.¹⁴ The pentaammineruthenium(III) coordination compounds were prepared from $(\text{NH}_3)_5\text{RuCl}_3^{15}$ following the general procedures previously described.^{1a,16} with the exceptions that pentane was used in

(1) Compilations of early references can be found in: (a) Hurst, J. K. *Biochemistry* **1979**, *18*, 1504-1510. (b) Norton, K. A., Jr.; Hurst, J. K. *J. Am. Chem. Soc.* **1982**, *104*, 5960-5966. (c) Hurst, J. K.; Lee, L. Y. C.; Grätzel, M. *Ibid.* **1983**, *105*, 7048-7056.

(2) Other recent pertinent studies include: (a) Harrington, P. C.; Wilkins, R. G. *J. Am. Chem. Soc.* **1981**, *103*, 1550-1556. (b) Winkler, J. R.; Nocera, D. G.; Yocom, K. M.; Bordignon, E.; Gray, H. B. *Ibid.* **1982**, *104*, 5798-5800. (c) Isied, S. S.; Worosila, G.; Atherton, S. J. *Ibid.* **1982**, *104*, 7659-7661. (d) McGourty, J. L.; Blough, N. V.; Hoffman, B. M. *Ibid.* **1983**, *105*, 4470-4472. (e) Lindsey, J. S.; Mauzerall, D. C.; Linschitz, H. *Ibid.* **1983**, *105*, 6528-6529. (f) Huddleston, R. K.; Miller, J. R. *J. Phys. Chem.* **1983**, *87*, 4687-4872. (g) Miller, J. R.; Peeples, J. A.; Schmitt, M. J.; Closs, G. L. *J. Am. Chem. Soc.* **1982**, *104*, 6488-6493. (h) Miller, J. R.; Hartman, K. W.; Abrash, S. *Ibid.* **1982**, *104*, 4296-4298. (i) Guarr, T.; McGuire, M.; Strauch, S.; McLendon, G. *Ibid.* **1983**, *105*, 616-618.

(3) DeVault, D.; Chance, B. *Biophys. J.* **1966**, *6*, 825-847. DeVault, D.; Parkes, J. H.; Chance, B. *Nature (London)* **1967**, *215*, 642-644.

(4) Hopfield, J. J. *Proc. Natl. Acad. Sci. U.S.A.* **1974**, *71*, 3640-3644.

(5) (a) Jortner, J. *J. Chem. Phys.* **1976**, *64*, 4860-4867. (b) Buhks, E.; Jortner, J. *J. Phys. Chem.* **1980**, *84*, 3370-3371. (c) Buhks, E.; Jortner, J. *FEBS Lett.* **1980**, *109*, 117-120.

(6) Ford, W. E.; Otvos, J. W.; Calvin, M. *Proc. Natl. Acad. Sci. U.S.A.* **1979**, *76*, 3590-3593.

(7) Tunuli, M. S.; Fendler, J. H. *J. Am. Chem. Soc.* **1981**, *103*, 2507-2513.

(8) Kurihara, K.; Sukigara, M.; Toyoshima, Y. *Biochim. Biophys. Acta* **1979**, *547*, 117-126.

(9) Runquist, J. A.; Loach, P. A. *Biochim. Biophys. Acta* **1981**, *637*, 231-244.

(10) Katagi, T.; Yamamura, T.; Saito, T.; Sasaki, T. *Chem. Lett.* **1982**, 417-420; **1981**, 503-506. Matsuo, T.; Itoh, K.; Takamura, K.; Hashimoto, K.; Nagamura, T. *Ibid.* **1980**, 1009-1012. Sudo, Y.; Kawashima, T.; Toda, F. *Ibid.* **1980**, 355-358.

(11) Ford, W. E.; Tollin, G. *Photochem. Photobiol.* **1982**, *35*, 809-819.

(12) Lee, L. Y. C.; Hurst, J. K.; Politi, M.; Kurihara, K.; Fendler, J. H. *J. Am. Chem. Soc.* **1983**, *105*, 370-373.

(13) Singleton, W. S.; Gray, M. S.; Brown, M. L.; White, J. L. *J. Am. Oil Chem. Soc.* **1965**, *42*, 53-56.

(14) Norton, K. A., Jr. Ph.D. Dissertation, Oregon Graduate Center, 1980.

(15) Glen, K.; Rehm, K. Z. *Anorg. Allg. Chem.* **1936**, *227*, 237-248.

place of diethyl ether to extract unreacted ligand from the crude $(\text{NH}_3)_5\text{Ru-4-Rpy}^{2+}$ product solutions,¹⁷ and the ions were then precipitated by adding saturated ethanolic solutions of ammonium hexafluorophosphate. The former modification avoided emulsification of solvent layers, and the latter minimized hydrolytic loss of ligand that otherwise occurred if aqueous solutions of precipitant were used. After oxidation with Ag(I), the Ru(III) complexes were isolated as their perchlorate salts. Electronic spectra were nearly identical with values previously reported for similar $(\text{NH}_3)_5\text{Ru-4-Rpy}$ complexes;^{18,14} spectral parameters (λ_{max} ($\log \epsilon_s$)) determined for $\text{R} = (\text{CH}_2)_{10}\text{CH}=\text{CH}_2$ are Ru(II), 408 (3.85), 245 (3.62) in ethanol; Ru(III), 251 (3.76) in 0.1 M TFA, 23 °C. The ultraviolet spectra gave no indication of the presence of ruthenium-containing impurities, e.g., $(\text{NH}_3)_5\text{RuCl}^{2+}$ or $(\text{NH}_3)_5\text{RuOH}^{2+}$ ions. The Ru(III) perchlorates are unstable, undergoing very slow color changes from pale yellow to gray to black over a period of several months. Their shelf life could be considerably extended by storing at -10 °C. Studies on the transmembrane diffusion properties of transition metal ions required synthesis of several coordination compounds, including $\text{K}_3\text{Co}(\text{C-N})_6$,¹⁸ $(\text{NH}_3)_3\text{Co}(\text{NO}_2)_3$,¹⁹ and $\text{K}[\text{Co}(\text{NO}_2)_2(\text{NH}_2\text{CH}_2\text{CO}_2)_2]$.²⁰ These preparations followed procedures described in the literature; spectroscopic properties of the purified complexes were nearly identical with reported values.

Reagent solutions of vanadous ion were prepared by reduction of vanadyl ion with amalgamated zinc in an argon atmosphere; the vanadyl solution was prepared by SO_2 reduction of V_2O_5 in dilute HClO_4 and standardized following permanganate oxidation to V(V) by reductive titration with Fe^{2+} ion using diphenylaminesulfonic acid as the indicator.²¹ Cuprous trifluoroacetate and chromous perchlorate solutions were prepared and standardized as previously described.¹⁶ Other chemicals were reagent grade and used without further purification. Aqueous solutions were prepared from water that was either doubly distilled from alkaline permanganate or purified by reverse osmosis ion exchange chromatography. Ascorbic acid was freshly prepared before use by dissolving weighed quantities into the reaction solvent.

Phosphatidylcholine Vesicle Formation and Characterization. Vesicles were formed by ultrasonic dispersal of aqueous suspensions of phosphatidylcholine for 2–3 h²² using the microtip probe of a Heat Systems-Ultrasonics Model W185F sonicator at a 70-W power setting. Typically, 80–100 mg of lecithin was used in 25 mL of 0.1 M sodium acetate or potassium acetate, pH 4.0, contained in a 50 mL round-bottomed flask. Various amphiphilic ruthenium(III) complexes were incorporated into the vesicles or other metal ions occluded within the inner aqueous phase by cosonication with the phospholipid suspension. Vesicle formation occurred more rapidly in the presence of the ruthenium(III) complexes, requiring only about 1.5 h sonication to achieve translucence, whereas the other ions had no apparent effect upon the process. The suspensions were purged of oxygen with a stream of nitrogen gas prior to sonication, which was then administered with constant N_2 flushing over the solution surface. The solutions were also cooled during sonication by immersion in an ice bath. These procedures effectively minimized oxidative degradation of the lecithin. The clarified suspensions were then centrifuged at 100 000 G and 4 °C for 195 min using a Beckman Ty65 fixed-angle rotor in a Model LS-65 instrument, and the fraction containing unilamellar vesicles²³ siphoned off. The vesicle suspensions were maintained at 4 °C and generally used within 24 h after preparation.

Vesicle concentrations in the suspensions were determined by adding known amounts of dipalmitoyl-L- α -phosphatidyl-[N -methyl-¹⁴C] choline (Amersham, 0.1 μCi) to the sonication mixture. Since this reagent was supplied dissolved in toluene/ethanol, the procedure adopted was to add an appropriate aliquot to the flask, evaporate solvent with a stream of nitrogen, and then follow with the normal procedures for vesicle preparation. Aliquots of the final vesicle suspensions were then mixed with Aquasol-2 scintillation fluid (1:9 v/v) and counted using a Beckman LS-3133P instrument. A standard [¹⁴C]phosphatidylcholine solution (2200 cpm) was used to ensure the accuracy of the counter readings. Yields of unilamellar liposomes isolated from the ultracentrifuged samples comprised about 30–40% of the added phospholipid.

(16) Norton, K. A., Jr.; Hurst, J. K. *J. Am. Chem. Soc.* **1978**, *100*, 7237–7242.

(17) Abbreviations used: bpy, 2,2'-bipyridine; CCCP, carbonyl cyanide *m*-chlorophenylhydrazone; PC, phosphatidylcholine; 4-Rpy, 4-(ω -alkenyl)pyridine; TFA, trifluoroacetic acid.

(18) Bigelow, J. H. *Inorg. Synth.* **1946**, *2*, 225–227.

(19) Schlessinger, G. *Inorg. Synth.* **1960**, *6*, 189–191.

(20) Celap, M. B.; Janjic, T. J.; Radanovic, D. *J. Inorg. Synth.* **1967**, *9*, 173–174.

(21) Price, H. J.; Taube, H. *Inorg. Chem.* **1968**, *7*, 1–9.

(22) Huang, C. *Biochemistry* **1969**, *8*, 344–352.

(23) Barenholz, Y.; Gibbes, D.; Litman, B. J.; Goll, J.; Thompson, T. E.; Carlson, F. D. *Biochemistry* **1977**, *16*, 2806–2810.

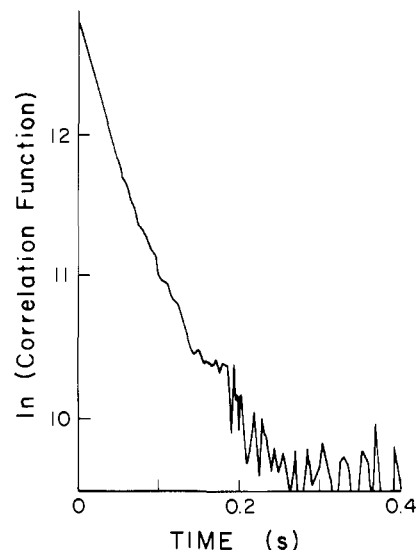


Figure 1. Autocorrelation decay curve for $(\text{NH}_3)_5\text{Ru-4-(11'-dodeceny)py}^{3+}$ -PC vesicles. Conditions: $[(\text{NH}_3)_5\text{Ru-4-Rpy}^{3+}] = 0.6 \mu\text{M}$, $[\text{PC}] = 10 \mu\text{M}$, in 0.01 M sodium acetate, pH 4.0.

Vesicle sizes were determined by photon correlation spectroscopy and electron microscopy. Time-averaged intensities of coherent light scattered from the particles were measured on a Chromatix KMX-6 photometer interfaced to a Langly-Ford autocorrelator.¹⁶ The autocorrelation function generated (Figure 1) was analyzed by the cumulants method,²⁴ which treats polydisperse systems. The Z -averaged particle diffusion coefficient (D) is calculated from the initial slope of the logarithmic plot, where the time constant $\tau_c = 1/2DK^2$,²⁵ with $K = (4\pi n/\lambda_0) \sin(\theta/2)$, n being the solution refractive index, λ_0 the incident light wavelength in vacuo, and θ the angle of scattered light; the variance (σ^2) is an index of polydispersity, i.e., the ratio of half-width at half-height to the average value of the distribution, which is calculated from the deviation of the experimental curve from simple exponential decay. Experimental parameters for our study were $n = 1.332$, $\lambda_0 = 633 \text{ nm}$, and $\theta = 4.5^\circ$. Assuming spherical symmetry, the hydrodynamic radii (R_H) of the vesicles can be calculated from the Stokes-Einstein equation, $D = kT/6\eta R_H$, where the solution viscosity, η , equals 8.90 mP. The system performance was periodically checked by analyzing nearly monodisperse suspensions of spherical latex particles having known radii. Electron micrographs were obtained using a Hitachi H6 11-BB microscope operating at 100 kV with the No. 2 polepiece inserted. Magnification factors were obtained from the appropriate intermediate lens current calibration curve. Samples were prepared by depositing a few drops of solution containing about 1 mM phospholipid on a 200-mesh copper grid which was supported by carbon or Formvar films. An absorbing filter paper was placed beneath the grid to facilitate sample dispersal on the surface. Immediately after sample deposition 1–2 drops of staining solution comprising 5% phosphotungstic acid in 70% ethanol was added to the grid surface.

Kinetic Methods. Rate measurements of the slow-phase reduction of vesicle-bound $(\text{NH}_3)_5\text{Ru-4-(11'-dodeceny)py}^{3+}$ ions, ligand hydrolysis, and perchlorate bleaching of the corresponding Ru(II) ion in homogeneous solution were made on a recorder-interfaced Cary 16 spectrophotometer. Temperature was controlled by circulating fluid from a thermostating bath through the instrument cell compartment. Typically, ice-cooled ruthenium-containing solutions were deoxygenated by passing a stream of chromous ion scrubbed argon through them for about 45 min; then a 2.3-mL aliquot was anaerobically syringe-transferred into an argon-flushed 1.0 cm path length cylindrical optical cell capped with a rubber septum. After several minutes was allowed for the solution to come to thermal equilibrium with the spectrophotometer, the reaction was initiated by syringe-transferring 0.2 mL of stock reductant solution into the cell. Absorbance changes were monitored at 415 nm for the ruthenium-vesicle suspensions and at 400 nm for the homogeneous systems. Visible spectra were recorded periodically over the time course of the reactions.

Fast-kinetic measurements were made on a Gibson-type stopped-flow instrument.¹⁶ Reactant solutions were prepared anaerobically in glass

(24) Koppel, D. E. *J. Chem. Phys.* **1972**, *57*, 4814–4820.

(25) Berne, B. J.; Pecora, R. "Dynamic Light Scattering"; Wiley: New York, 1976.

Table I. Vesicle Properties Determined by Photon Correlation Spectroscopy

vesicle ^a	[PC] (μM)	$[(\text{NH}_3)_5\text{Ru-4-Rpy}^{3+}]^b$ (μM)	$10^{-2}\tau_c$ (s) ^c	R_H (\AA) ^c	\bar{v}^c
lecithin (PC)	100		4.6 ± 0.2	245 ± 10	0.31 ± 0.02
lecithin (PC)	30		5.0	263	0.28
$(\text{NH}_3)_5\text{Ru-4-Rpy}^{3+}/\text{PC}$	100	5.9	4.4 ± 0.3	234 ± 14	0.34 ± 0.01
$(\text{NH}_3)_5\text{Ru-4-Rpy}^{3+}/\text{PC}$	100	22	4.3 ± 0.2	228 ± 11	0.44 ± 0.02

^a In 0.1 M sodium acetate (pH 4.0), ambient temperature. ^b R = 11'-dodecenylo moiety. ^c Ranges are average derivations from mean values for three separate preparations.

reservoirs which were attached to the instrument to permit direct loading into the drive syringes without exposure to air in the mixing block. Transmittance changes occurring upon mixing were stored on a Tektronix 549 oscilloscope and photographed for subsequent analysis.

Other Procedures. Qualitative studies of $(\text{NH}_3)_5\text{Ru-4-Rpy}^{3+}$ ion binding to the lecithin vesicles were made using gel chromatography. Sufficient Sephadex G-50 to make a 2×40 cm column was soaked overnight in distilled water, poured, and pre-equilibrated with buffer prior to introducing the vesicle suspensions. Eluted vesicles were collected in 2-mL fractions using a Gilson Model FC-80E fractionator operating in the drop-counting mode; the initial flow rate was adjusted to 1 mL/min. Column void volumes were determined by eluting blue dextran.

Membrane ultrafiltration studies were made by placing vesicle suspensions in a 47-mm filtration cell containing a prewetted Pellicon PSED semipermeable membrane (NMW cutoff 2.5×10^4 amu) and Teflon stirrer bar. The cell was attached to a Pellicon Carousel manifold and pressurized with N_2 gas to 20–25 psi. Under these conditions, the flow rate of the magnetically stirred solution was about 0.2 mL/min. Metal ion concentrations in the dilute ultrafiltration eluates and vesicle suspensions were determined by atomic absorption spectrometry using an Instrumentation Laboratories Model 551 spectrometer. This method proved unsuitable for determining the ruthenium content of vesicle-bound $(\text{NH}_3)_5\text{Ru-4-Rpy}^{3+}$ ions, however, because addition of lecithin vesicles to standard solutions of the complex caused an irreproducible twofold increase in the measured absorbances. In all other instances, vesicle addition caused no interference in the analysis. Samples were atomized in an air/acetylene flame. Detection wavelengths used for iron, cobalt, copper, and ruthenium were 373, 346, 218, and 350 nm, respectively; lamp currents were adjusted to 70–80% of the maximum allowed values to optimize sensitivity. For each metal ion analyzed, standard solutions of the metal complex ranging from 1 to 30 ppm were freshly prepared to obtain calibration curves, which were linear in all cases. Sample solutions were adjusted to lie within this range before measurement. Despite the bathochromic shift accompanying vesicle binding, absorbances at the wavelength maxima of the visible bands in equal concentrations of lecithin-bound and free $(\text{NH}_3)_5\text{Ru-4-Rpy}^{3+}$ ions are nearly identical (Figure 2); the concentration of the corresponding Ru(III) ion in prepared vesicle suspensions was therefore measured by optical spectroscopy following reduction to Ru(II) with excess ascorbate ion and assuming the value of the molar extinction coefficient measured in homogeneous solution.

Proton NMR spectra were recorded on a JEOL FX90Q spectrometer. Solution turbidities were measured with a Hach Model 2100A turbidimeter.

Results and Discussion

Physical Characterization of Phospholipid Vesicles. Logarithmic plots of autocorrelation decay functions obtained by quasielastic light scattering from lecithin vesicle suspensions were nonlinear, indicating some particle polydispersity; a representative curve is given in Figure 1. Hydrodynamic radii, determined from the initial slopes of the plots, and variances, determined from their curvatures, are listed in Table I. Although the average radii are unchanged within experimental error by binding of $(\text{NH}_3)_5\text{Ru-4-Rpy}^{3+}$ ions, the distribution of particle sizes increases slightly. The variances are not large,²⁶ suggesting that the vesicles are nearly monodisperse. The averaged hydrodynamic radii are not in good accord with vesicle sizes determined by microscopy, however. Electron micrographs show a nearly homogeneous population of approximately spherical vesicles with radii of 130 ± 15 \AA and a much smaller subpopulation comprising only a few percent of the total with radii of 353 ± 18 \AA , in comparison with the average radius of about 230 \AA measured by light scattering. This apparent

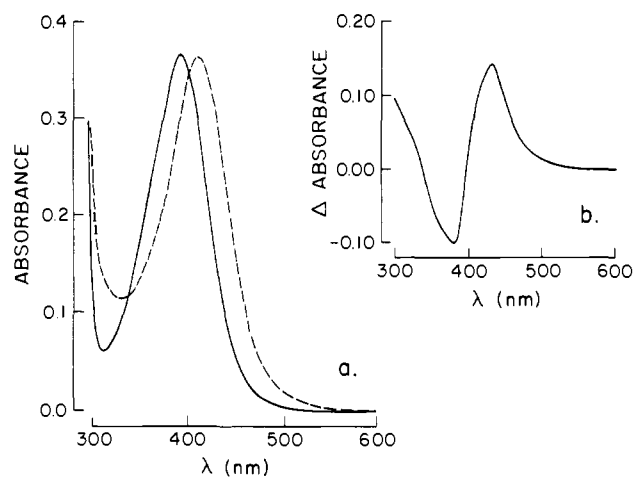


Figure 2. Optical absorption spectra of $(\text{NH}_3)_5\text{Ru-4-Rpy}^{2+}$ ions. (a) solid line, spectrum of $52 \mu\text{M}$ $(\text{NH}_3)_5\text{Ru-4-Rpy}^{2+}$ ion in 0.02 M sodium phosphate, pH 6.0; dashed line, spectrum under the same conditions in the presence of 3 mM PC vesicles. Graph b: $(\text{NH}_3)_5\text{Ru-4-Rpy}^{2+}/\text{PC}$ vs. $(\text{NH}_3)_5\text{Ru-4-Rpy}^{2+}$ difference spectrum, uncorrected for light scattering by the vesicles. The Ru^{2+} ion was generated in situ by ascorbate reduction of anaerobic solutions of the $(\text{NH}_3)_5\text{Ru-4-Rpy}^{3+}$ complex ion.

discrepancy can be resolved upon recognition that large particles are disproportionately strong light scatterers, strongly weighting the average radii determined from this property in polydisperse systems toward the larger values.^{26–29} For example, apparent radii determined by quasielastic light scattering spectroscopy for binary mixtures of small unilamellar (104 ± 15 \AA) and fused unilamellar (384 ± 4 \AA) vesicles were found to increase rapidly with admixture of small amounts of the larger particles; addition of less than 1% of the larger particles was sufficient to give a measured radius of about 250 \AA .²⁷ This distribution is very similar to that determined by electron microscopy in our studies. The sizes of the small unilamellar vesicles measured from the electron micrographs are consistent with previously reported values for sonicated lecithin suspensions;^{23,30} the larger particles are the same size as measured for aggregates of the small dipalmitoylphosphatidylcholine vesicles²⁷ or their fusion products.³¹ In general, fusion of small unilamellar phospholipid vesicles is thought to occur only from the relatively ordered lipid gel phase.^{31–34} Although egg lecithin vesicles are reported not to undergo appreciable fusion,³⁵ liposomes containing bound $(\text{NH}_3)_5\text{Ru-4-Rpy}^{3+}$ ions gave evidence of degradation upon prolonged aging (~ 12 h) at room temperature. The particles appeared stable at 4 $^\circ\text{C}$, but because this temperature

- (27) Wong, M.; Thompson, T. E. *Biochemistry* **1982**, *21*, 4133–4139.
 (28) Tricot, Y.-M.; Furlong, D. N.; Sasse, W. H. F.; Davis, P.; Snook, I.; Van Megen, W. J. *Colloid Interface Sci.* **1984**, *97*, 380–391.
 (29) Briggs, J.; Nicoli, D. F. *J. Chem. Phys.* **1980**, *72*, 6024–6030.
 (30) Huang, C.; Lee, L. *J. Am. Chem. Soc.* **1973**, *95*, 234–239.
 (31) Wong, M.; Anthony, F. H.; Tillack, T. W.; Thompson, T. E. *Biochemistry* **1982**, *21*, 4126–4132, and references therein.
 (32) Gaber, B. P.; Sheridan, J. P. *Biochim. Biophys. Acta* **1982**, *685*, 87–93.
 (33) Larrabee, H. L. *Biochemistry* **1979**, *18*, 3321–3326.
 (34) Petersen, N. O.; Chan, S. I. *Biochim. Biophys. Acta* **1978**, *509*, 111–128.
 (35) Taupin, C.; McConnell, H. M. In "Mitochondria: Biogenesis and Bioenergetics"; Van Den Bergh, S. G., Borst, P., Van Deenen, L. L. M., Riemersma, J. C., Slater, E. C., Tager, J. M., Eds.; North Holland/American Elsevier: 1972; pp 219–229.

(26) Chang, E. L.; Gaber, B. P.; Sheridan, J. P. *Biophys. J.* **1982**, *39*, 197–201.

Table II. Kinetic Summary of Slow-Phase Reduction of PC-Bound $(\text{NH}_3)_5\text{Ru-4-(11'-dodeceny)py}^{3+}$ Ion

reductant	$10^{-4}k$ (s^{-1}) ^d	% total optical change ^e (415 nm)	activation parameters ^f (ΔH^\ddagger , ΔS^\ddagger (23 °C))
Cr^{2+} (0.6–7.4 mM) ^a	6.7 ± 2.3	30 ± 3	13 kcal/mol, -29 eu
Cr^{2+} (0.6 mM) ^b	8.2 ± 1.7	29 ± 3	14 kcal/mol, -26 eu
Cr^{2+} (0.6 mM) ^c	12	31 ± 3	14 kcal/mol, -26 eu
V^{2+} (0.07–0.70 mM) ^a	12 ± 8.3	25 ± 3	9.9 kcal/mol, -38 eu
ascorbate (0.14–1.0 mM) ^a	12 ± 2.8	36 ± 5	11 kcal/mol, -34 eu

^a 3.4–7.5 mM PC, 0.14–0.4 mM $(\text{NH}_3)_5\text{Ru-4-Rpy}^{3+}$ in 0.1 M sodium acetate, pH 4.0. ^b 7 mM PC, 0.17 mM $(\text{NH}_3)_5\text{Ru-4-Rpy}^{3+}$, 7 μM valinomycin in 0.1 M potassium acetate, pH 4.0. ^c 7 mM PC, 0.17 mM $(\text{NH}_3)_5\text{Ru-4-Rpy}^{3+}$, 5 μM CCCP in 0.1 M potassium acetate, pH 4.0. ^d At 23 °C; ranges are average deviations from mean values for 2–11 individual runs. ^e Ranges are average deviations from mean values for 5–19 individual runs. ^f Temperature range 5–30 °C.

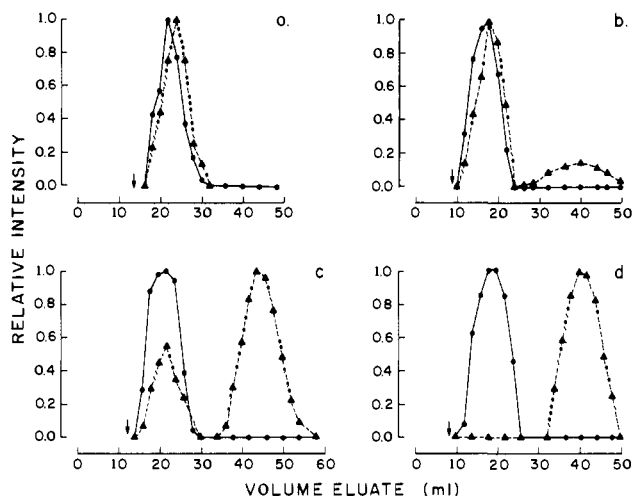


Figure 3. Elution profiles on Sephadex G-50 solution containing $(\text{NH}_3)_5\text{Ru-4-Rpy}^{3+}$ ions and PC vesicles. Suspensions of 3 mM PC were sonicated in 0.02 M sodium phosphate, pH 6.0, containing the concentrations of $(\text{NH}_3)_5\text{Ru-4-Rpy}^{3+}$ ions indicated below. After turbidity was measured, the complex ion concentrations of eluate fractions were determined as Ru(II) by ascorbate reduction under anaerobic conditions: (a) $[(\text{NH}_3)_5\text{Ru-4-(11'-dodeceny)py}^{3+}] = 23 \mu\text{M}$; (b) $[(\text{NH}_3)_5\text{Ru-4-(8'-noneny)py}^{3+}] = 28 \mu\text{M}$; (c) $[(\text{NH}_3)_5\text{Ru-4-(6'-hepteny)py}^{3+}] = 15 \mu\text{M}$; $[(\text{NH}_3)_5\text{Ru-4-(3'-buteny)py}^{3+}] = 14 \mu\text{M}$. Circles, relative turbidity; triangles, relative absorbance at 415 nm. The arrows indicate the column void volume determined with blue dextran.

borders upon the range (-12 to 5 °C) of the phosphatidylcholine gel \rightleftharpoons liquid crystalline phase transition,³⁶ the small number of larger particles detected could have arisen from vesicle fusion. Storage at the lowered temperature also minimized ligand hydrolysis of the added $(\text{NH}_3)_5\text{Ru-4-Rpy}^{3+}$ ions.³⁷

Adsorption of $(\text{NH}_3)_5\text{Ru-4-Rpy}$ Complex Ions. Strong binding of the $(\text{NH}_3)_5\text{Ru-4-(11'-dodeceny)py}^{3+}$ ion to the lecithin vesicles was evident from its chromatographic behavior on dextran gels (Figure 3a). The complex ion cochromatographed with the vesicles, which were excluded from the gel and appeared in eluate fractions immediately following the column void volume; in the absence of vesicles, the complex ion was retarded by the sieving action of the gel and appeared in subsequent fractions. The magnitude of the binding interaction diminished markedly with decreasing chain length of the ω -alkenyl pyridine substituent group (Figure 3); for $\text{R} = -(\text{CH}_2)_7\text{CH}=\text{CH}_2$ there is evidence of some unbound complex ion in the eluate, which progressively increases until, for $\text{R} = -(\text{CH}_2)_2\text{CH}=\text{CH}_2$, vesicles and complex ions are completely separable. Binding forces therefore arise predominantly by hydrophobic interaction of the hydrocarbon chain with the membrane internal lipid phase. The slight displacement of the elution band maximum of the complex ion from the vesicle band in Figure 3a is reminiscent of similar behavior in other ion-bound vesicle systems^{1c} and may represent some redistribution of ions during chromatography arising from dissociation from vesicles

(36) Ladbrooke, B. D.; Williams, R. M.; Chapman, D. *Biochim. Biophys. Acta* **1968**, *150*, 333–340.

(37) Ford, P. C.; Kuempel, J. R.; Taube, H. *Inorg. Chem.* **1968**, *7*, 1976–1983.

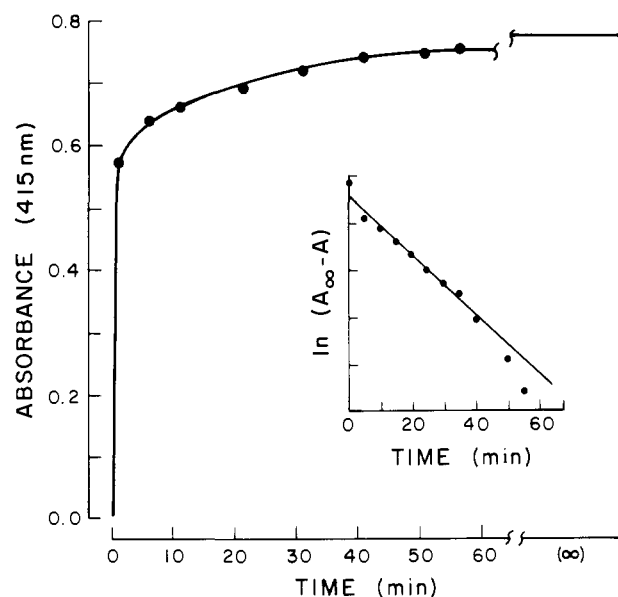


Figure 4. V^{2+} ion reduction of $(\text{NH}_3)_5\text{Ru-4-(11'-dodeceny)py}^{3+}$ -PC vesicles. Conditions: $[\text{V}^{2+}] = 0.68 \text{ mM}$, $[(\text{NH}_3)_5\text{Ru-4-Rpy}^{3+}] = 0.40 \text{ mM}$, $[\text{PC}] = 7.5 \text{ mM}$, in 0.1 M sodium acetate, pH 4.0, at 23 °C. Inset shows a logarithmic plot of the slow-phase reaction component, for which $k = 5.5 \times 10^{-4} \text{ s}^{-1}$.

on the leading edge of the band and readsorption by following vesicles.

Binding of the corresponding $(\text{NH}_3)_5\text{Ru-4-Rpy}^{2+}$ ions is most evident from the spectral shifts of the $\text{Ru}^{\text{II}}(\text{d}) \rightarrow \text{py}(\pi^*)$ optical bands which, being charge transfer in character,³⁸ are sensitive to medium polarity. For $\text{R} = -(\text{CH}_2)_{10}\text{CH}=\text{CH}_2$ (Figure 2) and $-(\text{CH}_2)_7\text{CH}=\text{CH}_2$, the apparent shifts are 15 and 8 nm, respectively, while, for $\text{R} = -(\text{CH}_2)_5\text{CH}=\text{CH}_2$, binding is apparent only from the appearance of a weak band in the complex ion-vesicle vs. complex ion difference spectrum, and, for $\text{R} = -(\text{CH}_2)_2\text{CH}=\text{CH}_2$, no spectral perturbation occurs upon vesicle addition. This order of interaction parallels the order for $(\text{NH}_3)_5\text{Ru-4-Rpy}^{3+}$ ion binding, substantiating the conclusion that binding is primarily attributable to the properties of the ω -alkenylpyridine ligands.

Kinetic Behavior of the Lecithin-Bound $(\text{NH}_3)_5\text{Ru-4-(11'-dodeceny)py}^{3+}$ Ion. Addition of various reducing agents in stoichiometric excess to solutions containing the complex ion bound to both inner and outer surfaces of the vesicles gave biphasic reduction to the $(\text{NH}_3)_5\text{Ru-4-(11'-dodeceny)py}^{2+}$ ion; a representative kinetic trace using vanadous ion as reductant is given in Figure 4. If the Ru^{III} complex ions are bound only to the external surface, just the fast-phase reduction step is observed; if the concentration of reductant is insufficient to completely reduce externally bound Ru^{III} , then the rapid appearance of the $\text{Ru}^{\text{II}}(\text{d}) \rightarrow \text{py}(\pi^*)$ visible band is followed by its slow bleaching, a consequence of reoxidation of Ru^{II} by perchlorate ion present in solutions (discussed below).

(38) Ford, P.; Rudd, D. F. P.; Gaunder, R.; Taube, H. *J. Am. Chem. Soc.* **1968**, *90*, 1187–1194.

For chromous, vanadous, and ascorbate ions in the 0.1 mM concentration range, the rapid-phase reduction rates are generally too great to detect by stopped-flow spectrophotometry, although reduction by Cu(I) is measurable. The magnitudes of these rates are consistent with rate behavior in homogeneous solution^{16,39} and suggest that the rapid phase corresponds to reduction of the externally bound, hence, directly accessible, ruthenium complex ions. Kinetic data for the slow-phase reactions are summarized in Table II. Measured rate constants varied over a twofold range from vesicle preparation to preparation under otherwise identical conditions. The basis for this relatively large uncertainty is presently unclear, although reactivity of these complex ions in homogeneous solution is known to be dramatically catalyzed by trace amounts of decomposition products.^{1a,1b} Slow-phase reduction by Cu(I) ion gave anomalous results characterized by complex irreproducible kinetic traces and a variable extent of reaction. Within the experimental uncertainty, slow-phase reduction by chromous, vanadous, and ascorbate ions is first order in complex ion and independent of both concentration and *identity* of the reductant. For these systems, relative amplitudes of the fast and slow steps are also independent of medium conditions at all temperatures studied. The marked rate retardation represented by the slow-phase reaction implies that a fraction of the complex ions, i.e., that initially bound to the inner membrane surface, is inaccessible to reductant. This interpretation is consistent with the relative stoichiometries of the two steps (Table II), assuming that the ruthenium(III) complex distributes uniformly over inner and outer surfaces during vesicle formation, since the inner surface area of spherical vesicles with an outer radius of 130 Å and bilayer width of 50 Å^{40,41} comprises about 28% of the total area. The slow step is attributable either to rate-limiting transmembrane diffusion of one of the reactants or to electron exchange between (NH₃)₅Ru-4-Rpy³⁺ and (NH₃)₅Ru-4-Rpy²⁺ ions bound to the opposite surfaces; direct transmembrane electron transfer between external reductant and (NH₃)₅Ru-4-Rpy²⁺ ion bound to the inner surface can be excluded from the form of the rate law and the independence of rate parameters upon the identity of the reductants (Table II).

Transmembrane Ion Diffusion. In general, phospholipid bilayer membranes have low ionic permeabilities as a consequence of the unfavorable Born charging energy required to transfer ions from the aqueous phase to the center of the hydrocarbon layer. Although ion transport across bilayers is slow in the absence of lipophilic carriers, rates are sensitive to various membrane structural parameters, increasing, e.g., with increasing carbon-carbon unsaturation and decreasing bilayer width,⁴² with increased dielectric constant of the lipid phase,⁴³ and with addition of oppositely charged surface groups.⁴⁴⁻⁴⁶ To gain some understanding of the ionic permeability of our systems, we examined the loss of hydrophilic trivalent transition metal ions entrapped within the vesicle inner aqueous phase. The ions used were hexacoordinate complexes whose overall charge was adjusted by varying the number of neutral and anionic ligands. The procedure adopted was to form the vesicles in solutions containing about 10 mM metal ions, then wash the external medium free of ions by repetitive batchwise filtration through a vesicle-impermeable membrane.⁴⁷ Typically, in one cycle, 40 mL of vesicle suspension was concentrated twofold and the lost solution replaced with 20 mL of

solvent; after 10 cycles, the metal ion concentration in the external medium had been diluted about 10³-fold, which was at the limits of detection by atomic absorption spectroscopy. The vesicle-containing fraction was then analyzed to determine its metal ion content; since the washing process required 3-4 h, the experiment measures the ability of the vesicles to retain the coordination complexes for a period of several times longer than the kinetic measurements. The integrity of the phospholipid vesicles over the course of the ultrafiltration experiments was confirmed by measurement of radioactivity in the suspensions containing the ¹⁴C-phospholipid-labeled vesicles.

We found that a significant fraction of the charged ions investigated ((NH₃)₅CoOH₂³⁺, Co(bpy)₃²⁺, Co(H₂O)₆³⁺, (NH₃)₅CoN₃²⁺, Co(NO₂)₂(gly)₂⁻, Co(CN)₆³⁻, Fe(CN)₆³⁻) could not be washed out of the vesicle-containing solutions, but that the neutral complex, (NH₃)₃Co(NO₃)₃, was reduced to concentration levels only slightly greater than anticipated from the cumulative dilution, inferring that it alone had diffused across the bilayer and become dialyzable.

Based upon an internal volume of 0.3 L/mol of phosphatidylcholine,⁴⁸ we calculate that the concentration of retained complex ions is an order of magnitude greater than initially added to the solution before sonication. This observation suggests that the ions adsorb weakly to the vesicle surface, e.g., as has been demonstrated by NMR methods for Ca²⁺ and La³⁺ ion binding to synthetic dipalmitoylphosphatidylcholine vesicles.⁴⁹ The magnitudes of occluded ions calculated assuming a simple binding isotherm and comparable association constants are very similar to measured values;⁴⁷ quantitative analysis is precluded because vesicle binding constants are not presently known. The complex ions, when added to the external medium of suspensions of preformed vesicles, were dialyzed from solution without evidence of retention; this result establishes that the retained ions are indeed compartmented within the inner aqueous phase of the vesicles. It appears, therefore, that under our reaction conditions the lecithin vesicles are impermeable to hydrophilic complex ions. These qualitative observations and the independence of rate constants on reductant identities (Table II) argue against the possibility that the slow-phase reduction step is attributable to transmembrane diffusion of the reductants; the different charge types alone would be expected to yield widely differing diffusion rates.

Transmembrane diffusion of the lecithin-bound (NH₃)₅Ru-4-(11'-dodeceny)py³⁺ ion was probed by examining as a function of time the redox behavior of vesicles initially containing only externally bound ion; implicit in the method is the assumption that the fast and slow phases measure the ion on the external and internal surfaces, respectively. Even when incubated for several hours at 25 °C, the Ru(III)-vesicle suspension showed no evidence of the slow-phase step upon reduction with either excess Cr²⁺ or ascorbate ion; the total amount of Ru(II) complex formed was unchanged over the time course of the measurements. Similarly, the bilayer permeability of the (NH₃)₅Ru-4-(11'-dodeceny)py²⁺ ion was investigated by reducing the Ru(III)-vesicles with Cr²⁺ ion, reoxidizing at various intervals with Fe(CN)₆³⁺ ion, then immediately reducing again with Cr²⁺ ion. After incubation for periods as long as 1 h at 25 °C as the Ru(II)-vesicle, cyclic oxidation-reduction showed no slow-phase component; greater than 90% of the original Ru(II) complex absorbance was recovered in the oxidation-reduction cycle. For both bound Ru(II) and Ru(III) complex ions, therefore, diffusion across the bilayer appears to be negligible on the timescale of the slow-phase reduction step.

From the observation that no change in absorbance of the vesicle-bound (NH₃)₅Ru-4-(11'-dodeceny)py²⁺ ions occurs within 7 h at 25 °C when reductant is present in excess, an upper limit to the rate of ligand aquation of $k \lesssim 10^{-6} \text{ s}^{-1}$ can be set. This number is smaller than reported values for aquation in homogeneous solution, e.g., for (NH₃)₅Ru-py²⁺ ion, $k \approx 3 \times 10^{-5} \text{ s}^{-1}$ at

(39) Gaunder, R. G.; Taube, H. *Inorg. Chem.* **1970**, *9*, 2627-2639.

(40) Huang, C.; Mason, J. T. *Proc. Natl. Acad. Sci. U.S.A.* **1978**, *75*, 308-310.

(41) Wilkins, M. H. F.; Blaurock, A. E.; Engelman, D. M. *Nature (London), New Biol.* **1971**, *230*, 71-76.

(42) See, e.g., Papahadjopoulos, D.; Nir, S.; Ohki, S. *Biochim. Biophys. Acta* **1972**, *266*, 561-583.

(43) Dilger, J. P.; McLaughlin, S. K. A.; McIntosh, T. J.; Simon, S. A. *Science* **1979**, *206*, 1196-1198.

(44) Papahadjopoulos, D.; Watkins, J. C. *Biochim. Biophys. Acta* **1967**, *135*, 639-652.

(45) McLaughlin, S. G. A.; Szabo, G.; Eisenman, G.; Ciani, S. M. *Proc. Natl. Acad. Sci. U.S.A.* **1970**, *67*, 1268-1275.

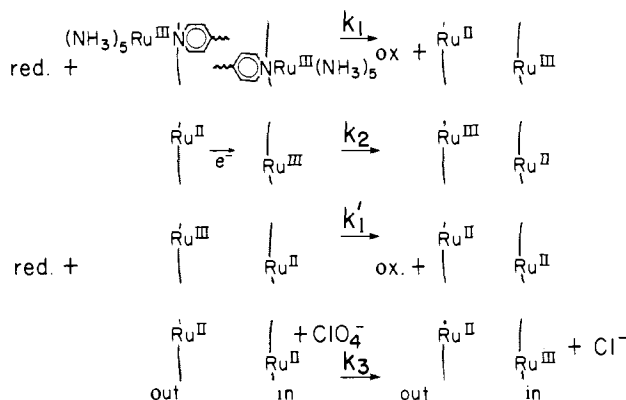
(46) Bangham, A. D.; Standish, M. M.; Watkins, J. C. *J. Mol. Biol.* **1965**, *13*, 238-252.

(47) Lee, L. Y. C. Ph.D. Dissertation, Oregon Graduate Center, 1984.

(48) Johnson, S. M.; Bangham, A. D.; Hill, M. W.; Korn, E. D. *Biochim. Biophys. Acta* **1971**, *233*, 820-826.

(49) Akutsu, H.; Seelig, J. *Biochemistry* **1981**, *20*, 7366-7373.

Scheme I



25 °C, $\mu = 1.0 \text{ M}$, extrapolated to pH 4.0,³⁷ suggesting that vesicle binding stabilizes the complex against ligand substitution by solvent.

Transmembrane Electron Transfer. Since mechanisms involving diffusion of reactants across the bilayer can be provisionally excluded, transmembrane redox must involve electron exchange between Ru(II) and Ru(III) complex ions bound to the opposite surfaces. A plausible kinetic sequence is given in Scheme I. Here, rapid reduction of externally bound Ru^{III} ion (k_1) is followed by slow transmembrane electron exchange (k_2), with the external Ru(III) ion formed being rapidly scavenged by excess external reductant (k_1'). The k_3 pathway represents the slow pseudo-first-order oxidation of internally bound Ru(II) by perchlorate ion. This complicating side reaction became apparent to us only upon observing bleaching of the Ru(II) chromophore in solutions of externally bound ruthenium ions with reductant as the limiting reagent.⁵⁰ Following bleaching, the vesicle-bound Ru(II) ion could be regenerated by adding reductant. Since $(\text{NH}_3)_5\text{Ru}-4-(11'$ -dodecenylyl) py^{3+} ion was isolated as its perchlorate salt, the perchlorate concentration in the reaction medium was $\sim 10^{-3} \text{ M}$. The rate constants for oxidation in homogeneous solution under these conditions fell within the range $k = 10^{-4}$ – 10^{-5} s^{-1} ; with V^{2+} ion as reductant, the rate constant increased linearly with perchlorate ion concentration, but was markedly less than first order for the other reductants. For vesicle-bound Ru(II), the rate constant for bleaching of the V^{2+} reduced particles was an order of magnitude less than in homogeneous solution. Based upon these observations, we estimate that $k_3 \leq 10^{-5} \text{ s}^{-1}$ for all reductants under the reaction conditions used for the redox studies. Perchlorate ion oxidation of other ruthenium(II) coordination compounds has been described.^{39,51}

In homogeneous solution, electron exchange between the Ru(II) and Ru(III) ions is first order in each reactant; assuming the same reaction order for transmembrane exchange, the rate law for reduction of Ru(III) complex ions on the inner surface is: $d[\text{Ru}^{\text{II}}]_i/dt = k_2[\text{Ru}^{\text{II}}]_o[\text{Ru}^{\text{III}}]_i - k_3[\text{Ru}^{\text{II}}]_i$, where the subscripts i and o refer to ions bound to inner and outer surfaces, respectively. When reductant is in excess, $[\text{Ru}^{\text{II}}]_o$ is constant since $k_1, k_1' \gg k_2$ and transmembrane diffusion of the bound ions does not occur. The rate equation is then homeomorphic with a reversible first-order approach to equilibrium, for which the pseudo-first-order rate constant, $k = k_2' + k_3$, with $k_2' = k_2[\text{Ru}^{\text{II}}]_o$. The transmembrane electron exchange step may not be second order however. Under certain conditions, bimolecular reactions which are constrained to a two-dimensional surface or compartmentalized in a solution microphase are expected on theoretical grounds to exhibit first-order kinetics.⁵² This effect has been demonstrated

(50) Perchlorate oxidation was also evident from the redox behavior of $(\text{NH}_3)_5\text{Ru}-4-(11'$ -dodecenylyl) py^{3+} ion over $\text{Zn}(\text{Hg})$. Only minute amounts of the reduced ions were generated in deoxygenated solutions containing 0.1 M ClO_4^- ion, as evident from the yellow color developing in the vicinity of the particles upon prolonged standing. Once removed from $\text{Zn}(\text{Hg})$, the color quickly disappeared. In contrast, in 0.1 M TFA, reduction was efficient and the Ru(II) complex formed was stable.

(51) Endicott, J. F.; Taube, H. *Inorg. Chem.* **1965**, *4*, 437–445.

experimentally in several instances.^{52–55} Although an adequate microscopic theory has not been developed which fits our experimental system, it is evident that if the ions are statistically correlated, e.g., as would occur if diffusion within the membrane plane and transfer to external surfaces of other vesicles were slow relative to transmembrane electron exchange, the system would behave as if electron transfer is intramolecular and give rise to first-order kinetics. Based upon estimates of the rates of lateral diffusion of phosphatidylcholine monomers in lecithin vesicles, for which the mean square displacement $\langle x^2 \rangle^{1/2} \geq 500 \text{ \AA s}^{-1/2}$,⁵⁶ an unconstrained amphiphilic Ru^{II} ion has access to the entire outer vesicle surface prior to transmembrane electron transfer, although randomization of the entire system by exchange of bound outer ions among the vesicles is not likely to occur on this timescale. At the highest ruthenium/phosphatidylcholine ratios used in these studies, there are about 170 Ru^{II} ions bound to the outer surface of each vesicle; in the absence of a stochastic theory directly applicable to these constraints, it is difficult to ascertain the reaction order. Alternatively, more complex mechanisms could also give rise to first-order behavior, e.g., if preferential alignment of complex ions occurred on the opposite vesicle surfaces so that membrane-separated "pairs" tended to form or if there existed a small number of saturable reactive sites on the membrane. Either circumstance might arise as a consequence of structural dislocations produced by ion binding that propagated through the bilayer. Our experimental results are consistent with a first-order process; measured transmembrane rate constants showed no systematic change when ruthenium/phosphatidylcholine ratios were varied over a fivefold range. The relative amplitudes of the two reaction steps were also unaffected by the level of vesicle doping by the Ru^{III} complex.

Transmembrane electron transfer is electrogenic; if charge transfer were to occur without any compensating ion migration, substantial transmembrane electrical potentials would develop; i.e., for the highest ruthenium/phosphatidylcholine ratios used in this study, complete reduction of internal Ru^{III} ions would generate a potential of about 1 V.⁴⁷ Standard reduction potentials for the $\text{V}^{3+/2+}$, $\text{Cr}^{3+/2+}$, and ascorbate/dehydroascorbate couples are -255 ,⁵⁷ -410 ,⁵⁷ and $+150 \text{ mV}$ (pH 4),⁵⁸ respectively; assuming a reduction potential for the vesicle-bound $(\text{NH}_3)_5\text{Ru}-4-(11'$ -dodecenylyl) $\text{py}^{3+/2+}$ couple similar to the solution potential for $(\text{NH}_3)_5\text{Ru}-\text{py}^{3+/2+}$ ions, i.e., 300 mV ,⁵⁹ the net chemical driving force for the various reductants is 150 – 710 mV . Clearly, in the absence of ion diffusion, electrical polarization of the membrane will increasingly oppose transmembrane reduction of internally bound Ru(III) ions as the reaction proceeds, ultimately limiting the extent of reduction in a manner dependent both upon the Ru/PC ratio and identity of reductant. Since neither of these effects are seen, charge-compensating ion flow must occur.

Ion diffusion might be rate limiting in the transmembrane redox step, although in the present case this possibility can be dismissed on kinetic grounds. Although the phospholipid bilayer is relatively impermeable to protons, passive diffusion occurs with a half-time of several minutes,^{60–62} which is the same order of magnitude as

(52) Hatlee, M. D.; Kozak, J. J.; Rothenberger, G.; Infelta, P. P.; Grätzel, M. *J. Phys. Chem.* **1980**, *84*, 1508–1519.

(53) Frank, A. J.; Grätzel, M.; Kozak, J. J. *J. Am. Chem. Soc.* **1976**, *98*, 3317–3321.

(54) Henglein, A.; Proske, T. *Ber. Bunsenges. Phys. Chem.* **1978**, *82*, 471–476.

(55) Rothenberger, G.; Infelta, P. P.; Grätzel, M. *J. Phys. Chem.* **1979**, *83*, 1871–1878.

(56) Kornberg, R. D.; McConnell, H. M. *Proc. Natl. Acad. Sci. U.S.A.* **1971**, *68*, 2564–2568.

(57) Latimer, W. M. "Oxidation Potentials"; Prentice-Hall: Englewood Cliffs, NJ, 1952.

(58) Clark, W. M. "Oxidation Reduction Potentials of Organic Systems"; Williams & Wilkins: Baltimore, MD, 1960.

(59) Lim, H. S.; Barclay, D. J.; Anson, F. C. *Inorg. Chem.* **1972**, *11*, 1460–1466.

(60) Biegel, C. M.; Gould, J. M. *Biophys. J.* **1981**, *33*, 102a.

(61) Nichols, J. W.; Deamer, D. W. *Proc. Natl. Acad. Sci. U.S.A.* **1980**, *77*, 2038–2042.

(62) Nichols, J. W.; Hill, M. W.; Bangham, A. D.; Deamer, D. W. *Biochim. Biophys. Acta* **1980**, *596*, 393–403.

observed for the transmembrane redox rate. Addition of the lipid-soluble proton carrier, carbonyl cyanide *m*-chlorophenylhydrazone (CCCP), to the vesicles to allow rapid passage of protons had no effect upon the redox rate constant; similarly, addition of the potassium ionophore, valinomycin, to suspensions containing K^+ as the electrolytic cation did not accelerate the slow-phase redox reaction. Therefore, it appears that k_2 measures rate-limiting electron exchange between the externally bound Ru(III) and internally bound Ru(II) ions; since k_3 is at least 10-fold less than the measured rate constant (k), it follows that $k_2 \approx k$ (Table II).

Electron-Transfer Distances. Since transmembrane redox exhibits simple exponential decay, reaction must occur over a single, well-defined distance.^{2f,g} Based upon the absence of detectable transmembrane diffusion of bound $(NH_3)_5Ru-4-(11'$ -dodeceny)pyridine(2+) ions within 1 h, the free-energy barrier imposed by the hydrocarbon interior of the bilayer is at least 24 kcal/mol at 23 °C. The chromophore is located in a nonpolar environment, however, since the bathochromic shift of its Ru(II) \rightarrow py charge-transfer band (λ_{max} 415 nm) is considerably greater than the shift observed on transferring the ion from water to ethanol ($\lambda_{max}(H_2O)$ 398 nm, $\lambda_{max}(EtOH)$ 408 nm). These observations suggest that the ions are held within the lipid phase near the interfacial boundary, their relatively deep potential wells being generated by opposition of dipolar image charge and hydrophobic forces in a manner analogous to that proposed for ionophoric complexes and "soft" organometallic ions.^{63,64} The distance of separation of the ions in this instance would then be nearly the full width of the hydrocarbon phase, i.e., about 40 Å.^{40,41} Electron transfer over distances of this magnitude is almost certainly nonadiabatic;^{5a} the reaction rate constant will therefore be limited by the probability of electron tunneling in the system.

Electrical conduction in multilayered films of axially aligned fatty acids has been adequately rationalized in terms of a theoretical model involving phonon-assisted tunneling to intermediary localized electron trapping sites,⁶⁵⁻⁶⁷ i.e.,

$$\tau^{-1} = \tau_0^{-1}(2\alpha l)^{3/2} \exp[-2\alpha l - (4\alpha/\pi N l k T)^{1/2}] \quad (1)$$

where $\alpha = (2m\phi)^{1/2}/\hbar$. This equation is adapted from a theory of impurity conduction in *n*-type semiconductors, in which electron transfer between nominally isoenergetic donor sites is driven by local field variations.⁶⁸ In the studies on layered Langmuir-Blodgett films, the effective tunneling distance (l) was found to be the width of a single fatty acid monolayer, implying that the interlayer electron trapping sites are located at the juncture of the hydrocarbon chains in adjacent layers,⁶⁹ and the energy of the electron at the top of the hydrocarbon barrier was found to be about 2.3 V below its energy in vacuo.⁶⁶ Partly as a matter of expedience, i.e., because the necessary experimental parameters are available from the planar film studies, we have attempted to fit the model to the vesicular systems as well. The vesicle bilayer is roughly approximated by two opposed monolayer films, for which $\tau_0 \approx 10^{-12}$ s, $N \approx 10^{15}$ cm⁻² V⁻¹, and the barrier height (ϕ) estimated from the Fermi energy of the Ru^{2+} ion in aqueous solution (-4.8 V)⁷⁰ is $\phi = 2.5$ V. Assuming that interlayer trapping sites are also present at the intersection of the hydrocarbon surfaces in the vesicle, the effective electron-transfer distance is slightly

(63) Anderson, O. S.; Fuchs, M. *Biophys. J.* **1975**, *15*, 795-830.

(64) Ketterer, B.; Neumcke, B.; Luger, P. *J. Membr. Biol.* **1971**, *5*, 225-245.

(65) Iizima, S.; Sugi, M. *Appl. Phys. Lett.* **1976**, *28*, 548-549. Sugi, M.; Fukui, T.; Iizima, S. *Appl. Phys. Lett.* **1975**, *27*, 559-561.

(66) Seefeldt, K.-P.; Mobius, D.; Kuhn, H. *Helv. Chim. Acta* **1977**, *60*, 2608-2632.

(67) Kuhn, H. *Pure Appl. Chem.* **1979**, *51*, 341-352.

(68) Miller, A.; Abrahams, E. *Phys. Rev.* **1960**, *120*, 745-755.

(69) See also: (a) Sugi, M.; Fukui, T.; Iizima, S. *Chem. Phys. Lett.* **1977**, *45*, 163-166. (b) Sugi, M.; Nembach, K.; Mobius, D. *Thin Solid Films* **1975**, *27*, 205-216. (c) Sugi, M.; Nembach, K.; Mobius, D.; Kuhn, H. *Solid State Commun.* **1974**, *15*, 1867-1870.

(70) The Fermi energy (ϵ) is related to the standard reduction potentials (E_0) by $\epsilon = -E_0 - 4.5$ V,⁶⁶ where -4.5 V is a measure of the energy difference between the free electron and the standard hydrogen electrode. For $(NH_3)_5Ru-4-Rpy^{3+/2+}$, $E_0 \approx 0.30$ V,¹⁶ giving $\epsilon = -4.8$ V.

larger^{68,69} than the width of the outer monolayer; i.e., $d \approx 20-22$ Å.⁴⁰ Using these parameters, the electron tunneling relaxation rate constant (τ^{-1}) is calculated to be $\tau^{-1} = 0.1-1.8 \times 10^{-2}$ s⁻¹ at 23 °C. This value is very nearly equal to the experimentally measured transmembrane redox rate constant (Table II).

Temperature Dependence of the Transmembrane Redox Reaction. Equation 1 predicts that the relaxation times for electron tunneling will be nearly temperature independent, assuming that the barrier parameters are also invariant with temperature.^{69a} From 5 to 30 °C, the relaxation rate constant is calculated to increase about 20%, although we observe a six- to sevenfold increase over the same temperature range. Activation parameters reported in Table II are best-fit values determined using the theory of absolute reaction rates; it should be recognized that the narrow experimentally accessible temperature range precludes unambiguous identification of the functional form of the temperature dependence of the rate constants.

Phospholipid bilayers undergo lateral expansion with increasing temperature; this effect is most pronounced at the gel \rightleftharpoons liquid crystalline-phase transition, but also occurs in the separate phases above and below the transition region.⁷¹⁻⁷⁴ One consequence of this expansion is that the barrier width decreases; the linear expansion coefficient (α), where $\alpha = \partial l/\partial T$, is about -0.01 deg⁻¹ for dimyristoylphosphatidylcholine vesicles in their fluid phase⁷¹ and is -0.003 deg⁻¹ for lamellar brain phospholipid.⁷² In our system, α need only be -0.003 deg⁻¹ to account for the magnitude of the observed temperature-dependent changes in the rate constants.⁷⁵ Since this is within the magnitude of change measured in the other bilayer systems, it is reasonable to ascribe the temperature dependence of the reaction predominantly to the variations in barrier width, i.e., electron-transfer distances. The dominant effect of varying l in eq 1 appears in the $\exp(-2\alpha l)$ term; if l varies approximately linearly with temperature, then the temperature dependence upon the rate constant will exhibit Arrhenius-type behavior. In summation, it appears that the "hopping" conduction model⁶⁵⁻⁶⁹ is capable of accounting for the experimentally observed transmembrane redox rate behavior.

Conceptual Problems. Recent developments in the theory of nonadiabatic electron transfer suggest that electron-tunneling probabilities are controlled by vibronic coupling to high-frequency normal modes comprising the intramolecular vibrations of the donor and acceptor centers, with coupling to low-frequency medium phonon modes making relatively minor contribution.^{4,5} Accordingly, there should exist a substantial Franck-Condon barrier to electron tunneling at ambient temperatures, but this "nuclear" term is not evident from either the absolute magnitude of the rate constant⁷⁶ or its temperature dependence, the dominant contribution to which appears to arise from bilayer thinning. Activationless electron transfer has been observed in several primary charge separation steps in bacterial photosynthesis,^{5c} however, and, as mentioned, in intramolecular electron transfer in a synthetic $Ru^{II}-(Fe^{III})$ cytochrome *c* binuclear ion.^{2b,c} Each of these reactions is only weakly exoergic ($\Delta E^\circ \approx 200-400$ mV). Apparently, the present system also belongs to this small class of anomalous reactions.

"Hopping" conduction, as has been applied to vesicular assemblies, implies transfer of electronic charge to discrete acceptor sites within the hydrocarbon phase. For net transmembrane redox to occur at an appreciable rate, these sites must be nearly

(71) Watts, A.; Marsh, D.; Knowles, P. *Biochemistry*, **1978**, *17*, 1792-1801.

(72) Luzzati, V.; Husson, F. *J. Cell Biol.* **1962**, *12*, 207-218.

(73) Marsh, D. *Biochim. Biophys. Acta* **1974**, *363*, 373-386.

(74) Trauble, H.; Haynes, D. H. *Chem. Phys. Lipids* **1971**, *7*, 324-335.

(75) Egg lecithin bilayers undergo a relatively broad phase transition at -12 to 5 °C;³⁶ correspondingly, the vesicles are in their fluid phase over the temperature range investigated.

(76) Given that the experimental tunneling parameters are only approximate, it is difficult to make quantitative comparison of τ^{-1} and k_2 . For example, the value chosen for τ_0 may be 10-fold too large;⁶⁶ if so, the tunneling rate calculated from eq 1 would be $\tau^{-1} = 0.2$ s⁻¹. The 200-fold lower rate constant for transmembrane redox ($k_2 = 10^{-3}$ s⁻¹) might then be attributed to a small Franck-Condon factor.

isoenergetic with the Ru²⁺ Fermi level. This condition requires that their energy levels be about 2.5 V below the Fermi level of the hydrocarbon chain. It is difficult to imagine, however, the sort of molecular organization that would lead to orbital stabilization to this extent. Ultimately, electron transfer may prove to be more appropriately described in terms of superexchange-type coupling mechanisms, e.g., as discussed by Jortner.^{5a} In this regard, both the phosphatidylcholine monomers and alkyl substituent chain of the ruthenium coordination complex used in these studies possess olefinic unsaturation, the relatively low-lying unoccupied orbitals of which might engage in electronic mixing with donor and acceptor orbitals. Current research is directed

at characterizing the rate-influencing factors inherent in the ligand and membrane molecular structures.

Acknowledgment. Financial support was provided by the U. S. Public Health Service (Grant GM-20943) and U.S. Department of Energy (Contract DE-AC06-83ER13111). Light-scattering measurements were made in the laboratory of Professor Michael Grätzel (Lausanne, Switzerland), to whom we are indebted for his generosity and hospitality.

Registry No. (NH₃)₅RuL³⁺ (L = 4-(11'-dodeceny)pyridine), 92669-57-3; Cr, 7440-47-3; V, 7440-62-2; ascorbic acid, 50-81-7; dipalmitoyl-L- α -phosphatidylcholine, 63-89-8.

Infrared Spectra of MeMn(CO)₅ and MeRe(CO)₅ Species: Methyl Group Geometry and the Effects of Internal Rotation

C. Long,^{1a} A. R. Morrisson,^{1b} D. C. McKean,* and G. P. McQuillan

Contribution from the Department of Chemistry, University of Aberdeen, Aberdeen AB9 2UE, Scotland. Received June 14, 1984

Abstract: Infrared spectra in the CH and CD stretching regions are reported for various MeMn(CO)₅ and MeRe(CO)₅ species. Interpretation is made in terms of a freely internally rotating methyl group whose individual bond-stretching force constants vary during the rotation. The "average" "isolated" CH stretching frequencies of 2955.0 and 2934.6 cm⁻¹ observed in the CHD₂ spectra are used to predict r_0^{CH} values of 1.095, Å (Mn) and 1.098₀ Å (Re), respectively, HCH angles, A_0 , and $D^\circ_{298}(\text{C-H})$ values. The CH bonds are of medium strength, that in the Re compound being slightly weaker than the Mn one and displaying an inverse relationship to $D(\text{M-CH}_3)$.

The methyl pentacarbonyls of manganese and rhenium have been the subject of a number of structural studies, involving gas-phase electron diffraction^{2,3}, X-ray diffraction and incoherent inelastic neutron scattering,⁴ and vibrational spectroscopy.⁴⁻⁸ These have left uncertain two structural features associated with the methyl group, its geometry, and its internal rotational motion. The disordered structure of the Mn crystal meant that no geometric information could be obtained from the X-ray study, while the hydrogen positions were not located by the electron-diffraction experiments.^{2,3} This situation may be remedied through a study of the CH stretching region of the CHD₂ species, from whose "isolated" CH stretching frequencies, bond lengths and HCH angles may be predicted by the use of correlation graphs.^{9a,b}

Prior evidence relating to the internal rotation problem in the Mn compound is of three kinds. A Raman line at 174 cm⁻¹ and part of a broad IINS feature at 169 cm⁻¹, both in the crystal at 10 K, have been assigned to a torsional mode of the CH₃ group.⁴ As discussed below, this would be impossible with a V_{12} potential term and would require a high barrier of >350 cm⁻¹ with a V_4 one. The second and third observations are from infrared spectra and apparently conflict with each other. The antisymmetric

stretching mode of the methyl group is split into two components in the gas phase, while in solution and in the solid it presents a single broad band whose width varies little with temperature.⁶ The latter observation leads to an estimate of the barrier height of 944 ± 175 cm⁻¹.²⁴

Here again the infrared study of partially deuterated species may throw some light, at the cost, however, of introducing a further complication. Previous work in this field^{8a} has revealed a variety of circumstances in which CH bonds within a methyl group vary in strength according to their angular position within the molecule. Where internal rotation is restricted, these have straightforward effects in the spectra. Infrared bands appear at frequencies corresponding to bonds in each of the various potential minima. However, for the case of low barriers, as in MeNO₂, MePh,^{10,11} MeBF₂, MeBCl₂, Me₃B, and (MeBO)₃,¹² the spectra and their interpretation are more complex. Theoretical treatments of a CH₃ group and of a CHD₂ one rotating against an infinitely heavy, planar skeleton, as in the above molecules, have been given by Sheppard and Woodman¹³ and Cavagnat and Lascombe¹¹ (hereafter SW and CL, respectively).

Taken together, this prior work yields strong evidence for a variation of CH bond strength during the essentially free internal rotation in the above cases. While no corresponding theory exists for the vibration-rotation transitions of a methyl group rotating against a C_{4v} skeleton, as in the pentacarbonyls, features similar to the earlier ones may reasonably be expected to occur if the barrier is likewise very low. Since this work is little known, it will be necessary to give a more detailed review of it before we can conduct a meaningful discussion of the pentacarbonyl spectra.

(1) (a) Present address: National Institute for Higher Education, Dublin 9, Ireland. (b) Present address: Robert Gordon's Institute of Technology, St. Andrew St., Aberdeen, Scotland.

(2) Seip, H. M.; Seip, R. *Acta Chem. Scand.* **1970**, *24*, 3431.

(3) Rankin, D. W. H.; Robertson, A. *J. Organomet. Chem.* **1976**, *105*, 331.

(4) Andrews, M. A.; Eckart, J.; Goldstone, J. A.; Passell, L.; Swanson, B. *J. Am. Chem. Soc.* **1983**, *105*, 2262.

(5) McHugh, T. M.; Rest, A. J. *J. Chem. Soc., Dalton Trans.* **1980**, 2323.

(6) Dempster, A. B.; Powell, D. B.; Sheppard, N. *J. Chem. Soc. A* **1970**, 1129.

(7) Hieber, W.; Braun, G.; Beck, W. *Chem. Ber.* **1960**, *93*, 901.

(8) For a more complete set of references to vibrational spectra of the Mn compound, see ref 4. Reference 7 is the only source known to us of data for the $\nu(\text{CH})$ region of CH₃Re(CO)₅.

(9) McKean, D. C. *Chem. Soc. Rev.* **1978**, *7*, 399. (b) McKean, D. C. *J. Mol. Struct.* **1984**, *113*, 251.

(10) McKean, D. C.; Watt, R. A. *J. Mol. Spectrosc.* **1976**, *61*, 184.

(11) Cavagnat, D.; Lascombe, J. *J. Mol. Spectrosc.* **1982**, *92*, 141.

(12) McKean, D. C.; Becher, H. J.; Bramsiepe, F. *Spectrochim. Acta, Part A* **1977**, *33A*, 951.

(13) Sheppard, N.; Woodman, C. M. *Proc. R. Soc. London, Ser. A* **1969**, *A313*, 184.